Drug Metab Drug Interact 2012;27(1):47–54 © 2012 by Walter de Gruyter • Berlin • Boston. DOI 10.1515/dmdi-2011-0034

The microstructure of DNA - egg yolk phosphatidylcholine - gemini surfactants complexes: effect of the spacer length

[1]Daniela Uhríková*, [1]Petra Pullmannová, [1]Adriana Šabíková, [2]Ferdinand Devínsky, [3]Sergio S. Funari

[1]Department of Physical Chemistry of Drugs, Faculty of Pharmacy, Comenius University, Odbojárov 10, 832 32 Bratislava, Slovakia

[2]Department of Chemical Theory of Drugs, Faculty of Pharmacy, Comenius University, Odbojárov 10, 832 32 Bratislava, Slovakia

[3]HASYLAB at DESY, Notkestr. 85, D-22607 Hamburg, Germany

*Corresponding author: Tel. +421250117292

E-mail address: uhrikova@fpharm.uniba.sk (D. Uhríková)

Short title: The microstructure of DNA – EYPC – CnGS complexes

Number of words: 6125

Figures: 5

Tables: 0

References: 58

Abstract:

The microstructure of complexes DNA – egg yolk phosphatidylcholine (EYPC) – alkane-α,ω-diyl-bis(dodecyldimethylammonium bromides) (CnGS, spacer n = 2–12, n is even) was studied using small angle X-ray diffraction. At EYPC:CnGS = 1:1 mol/mol, the condensed lamellar phase was identified in complexes with CnGS, n = 2–4, while longer spacer ($n \geq 6$) induced a hexagonal phase. The condensed lamellar phase L_α^c was observed in the range $2 \leq$ EYPC:GnGS ≤ 10 (mol/mol) in all complexes. The distance between adjacent DNA strands increases linearly with decreasing surface charge density of EYPC-CnGS vesicles. We determined the increase in d_{DNA} 0.40 ± 0.03 nm *per* 1 mol of EYPC from the slope of $d_{DNA} = f$(molEYPC/molCnGS) in the range of molar ratios 2≤EYPC:CnGS≤5. At lower surface charge density, EYPC:CnGS > 5 mol/mol, the lenght of CnGS spacer (n = 6–10) modulates the DNA-DNA distance.

Key words: lipoplexes - gemini surfactants – DNA – egg yolk phosphatidylcholine – small angle X-ray diffraction

Abbreviations:

GS gemini surfactants; CnGS gemini surfactants alkane-α,ω-diyl-bis(dodecyldimethylammonium bromides); EYPC egg yolk phosphatidylcholine; DOPE dioleyphosphatidylethanolamine; DNA deoxyribonucleic acid; R_4N^+ cationic ammonium headgroup; SAXD small angle X-ray diffraction; L_α^C condensed lamellar phase; H_{II}^C condensed inverted hexagonal phase.

Introduction

Gemini surfactants (GS) are amphiphilic molecules containing two head groups and two aliphatic chains linked by a spacer. They typically show greatly enhanced surfactant properties relative to the corresponding monomeric surfactants. In addition to the synthesis of "bisquaternary ammonium salts", as gemini surfactants were also termed (1), the relationship between their structure, surface activity and micelle formation was extensively studied at our faculty (see e.g. (2-5)). They are potent as plasmid curing agents (6), and were used to increase the efficiency of the DNA transfer into bacterial cells (7). Gemini surfactants have been intensively investigated as possible vectors for gene transfection (8-10). A majority of almost 250 GS compounds tested in (11) of 20 different structural types showed very good transfection activity *in vitro*.

Cationic liposomes as gene delivery carriers were used for the first time by Felgner et al (12). Since the first study, many cationic lipids have been synthesized, and physico-chemical properties, structure, and transfection efficiency have been intensively investigated. It was found that helper neutral lipid used together with cationic components moderates the colloidal and structural properties of the complex and facilitates the transport through the cell's membrane (13-15). However, their transfection efficiency, both *in vitro* and *in vivo*, depends in a rather complex way on different interconnected parameters, ranging from the chemical composition of the lipid components to the size and size distribution of the complexes, their surface charge and, to the composition of the suspending medium (see e.g. 16).

Within this study we use the simple type of GS alkane-α,ω-diyl-bis(alkyldimethylammonium bromide) (CnGSm, where n = 2–12 is the number of spacer carbons and m = 12 is the number of alkyl tails carbons) (Figure 1). This study is focused on the role of GS spacer in DNA packing. The length of alkyl chains was chosen constant for all CnGS homologues (m=12) to minimize the number of variables in the system. Complexes CnGS12 – dioleyphosphatidylethanolamine (DOPE) – DNA have been tested as gene delivery carriers for somatic cells *in vitro* (17) and *in vivo* (18). For the CnGS12, n = 3–16, no transfection was observed in the absence of helper lipid. Transfection efficiencies were shown to be greatest for spacers of $n \leq 4$ or $n > 12$. It has been found that the character of spacer plays a role in the transfection efficiency of DNA complexes based on GS also in (19-22). Generally, GS with short length of spacer were reported in regards their enhanced transfection activity.

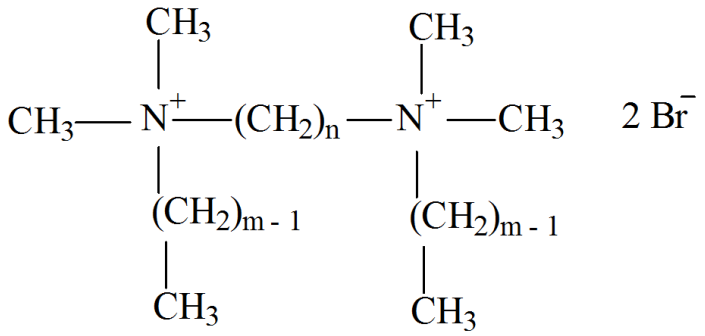

Fig. 1 The structure of alkane-α,ω-diyl-bis(alkyldimethylammonium bromide) (CnGSm).

From physico-chemical view, cationic vesicles interact with DNA polyanion forming string-like colloidal particles of an ordered internal microstructure (23,24). Several types of internal arrangement in CnGSm-phospholipid-DNA complexes have been identified using small angle X-ray diffraction: the condensed lamellar phase L_{α}^{C} with ordered DNA monolayers intercalated between lipid bilayers (17,25,26), the condensed inverted hexagonal phase H_{II}^{C} with linear DNA molecules surrounded by lipid monolayers forming inverted cylindrical micelles arranged on a hexagonal lattice (27-29) and, cubic phases (17,30) were reported as well.

In this study, the experimental conditions (design of the gemini surfactant molecule, ionic strength, charge ratios) were chosen with the aim to simplify the system and to shed more light into understanding of the principle of DNA packing by gemini surfactants intercalated in the phospholipid bilayer. We employ small angle X-ray diffraction (SAXD) to follow the microstructure of complexes formed due to DNA interaction with cationic vesicles prepared as a mixture of egg yolk phosphatidylcholine (EYPC) and gemini surfactants CnGS as a function of the length of spacer, n = 2–12, n is even. Complexes were prepared at isoelectric point (ratio of positive CnGS/negative DNA charges equal to 1) estimated by calculation based on nominal charges of CnGS and DNA. The experiment was focused on a role of the CnGS spacer length in the DNA packing in a condensed lamellar phase as a function of surface charge density. SAXD identified L_{α}^{C} phase in a large range of molar ratios 2 ≤ EYPC:CnGS ≤ 10 without demixing of components. Our previous study (28) has revealed difference in the DNA packing at two spacer lengths n = 2 and 10 that motivated us to extend the experiment.

Materials and methods

Highly polymerized calf thymus DNA (Sigma-Aldrich Co., St. Luis, Missouri, USA) was dissolved in 1.5 mM NaCl, pH~7, at concentration ~2 mg/ml. The precise value of DNA concentration was determined spectrophotometrically (Hewlett Packard 8452A Diode array spectrophotometer, Hewlett Packard, Palo Alto, California, USA), according to equation: $c_{DNA} = A_{260} \,.\, 4.7 \,.\, 10^{-5}$ (g/ml), where A_{260} is the absorbance at wavelength λ = 260 nm. The concentration of DNA is referred as molar concentration of DNA base pairs (mol bp). The purity of DNA was checked by measuring the absorbance A_λ at λ = 260 nm and 280 nm, we have obtained A_{260}/A_{280} = 1.8. Alkane-α,ω-diyl-bis(dodecyldimethylammonium bromide), CnGS n = 2–12, were prepared as described in (1) and purified by manifold crystallization from a mixture of acetone and methanol. Aqueous solutions of CnGS were prepared using the same solvent (1.5 mM NaCl, pH ~ 7). Phosphatidylcholine from hen egg yolks (EYPC) was prepared, purified and analysed by thin layer chromatography according to Singleton et al. (31). Its molecular weight of 779.7 g/mol was calculated from the chemical composition of its acyl chains (32). EYPC was dispersed at 25.9 mM concentration (in 1.5 mM NaCl, pH ~ 7). The dispersion was vortexed and homogenized by sonication in an ultrasound bath (Sonorex Bandelin, Bandelin electronic GmbH&Co. KG, Berlin, Germany) and by freezing-thawing process. From the dispersion of multilamellar liposomes, extruded unilamellar liposomes were prepared according to MacDonald et al. (33) using the LiposoFast Basic extruder (Avestin, Ottawa, Ontario, Canada). The multilamellar liposomes were extruded through polycarbonate filter (accessory of the extruder, Avestin, Ottawa, Ontario, Canada) with pores of diameter 100 nm mounted in the extruder fitted with two gas-tight Hamilton syringes (accessory of the extruder, Hamilton, Reno, Nevada, USA). The sample was subjected to 51 passes through the filter at room temperature.

EYPC unilamellar vesicles and CnGS solution were mixed at appropriate volume ratios to obtain the required molar ratio of EYPC:CnGS. The amount of CnGS (~1 mg) was kept constant in each sample. The sample was vortexed for a short time and DNA solution was added reaching the required ratio DNA:CnGS = 1:1 mol bp/mol. The sample was again vortexed for a short time. The sediment was created in the sample after few minutes (~ 30 min). Before measurement, the sample was shortly centrifuged, and the sediment was placed between two Kapton foil (Dupont, CMC Klebetechnik GmbH, Frankenthal, Germany) windows of a sample holder for X-ray diffraction.

Small- (SAXD) and wide-angle (WAXD) synchrotron radiation diffraction experiments were performed at the soft condensed matter beamline A2 at HASYLAB at the Deutsches Elektronen Synchrotron (DESY) in Hamburg (Germany), using a monochromatic radiation of wavelength λ = 0.15 nm. The evacuated double-focusing camera was equipped with two linear delay line readout detectors. The sample was equilibrated at selected temperature (20 °C) for 5 min before exposure to radiation. The raw data were normalized against the incident beam intensity using the signal intesity measured in the ionization chamber. The SAXD detector was calibrated using rat tail collagen (34) and the WAXD detector by tripalmitin (35,36). Each diffraction peak of SAXD region was fitted with a Lorentzian above a linear background. The WAXD pattern (not shown in the figures) of all measured samples exhibited one wide diffuse scattering characteristic for liquid-like carbon chains of phospholipid and CnGS molecules.

Results and Discussion

When a solution of cationic surfactant CnGS is added to the dispersion of unilamellar EYPC vesicles, molecules of surfactant intercalate between zwitterionic EYPC molecules and the surface becomes positively charged (37). Cationic EYPC – CnGS vesicles interact with DNA forming colloidal particles with an internal ordered microstructure. We have employed SAXD to examine the microstructure of DNA-EYPC-CnGS complexes. Figure 2 shows representative SAX diffractograms of complexes formed due to DNA interaction (DNA:CnGS=1:1 mol bp/mol) with cationic vesicles prepared at low volume fraction of EYPC, at molar ratios EYPC:CnGS=1:1 and EYPC:C2GS=2:1. Multilamellar EYPC vesicles were used as reference sample (Figure 2). Two diffraction peaks, $L(1)$ and $L(2)$, whose ratio between s values of their maxima is L(2)/L(1)=2 represent typical diffraction pattern of a lamellar phase. We determined the repeat distance $d = 1/s_1 = 6.53 \pm 0.01$ nm from the first peak maximum. DNA-EYPC-CnGS complexes with a short length of spacer, $n < 6$ show lamellar organization (Fig. 2). We found the periodicity $d = 6.15 \pm 0.01$ nm for the lipid bilayer stacking of DNA-EYPC-C2GS complex at molar ratio EYPC:C2GS=1:1, however the diffractogram gives no information about any regularity in DNA strands packing. Diffractogram in the Figure 2, obtained from the complex prepared at EYPC:C2GS=2:1 mol/mol, shows in addition to two peaks related to EYPC-C2GS bilayers organized in the

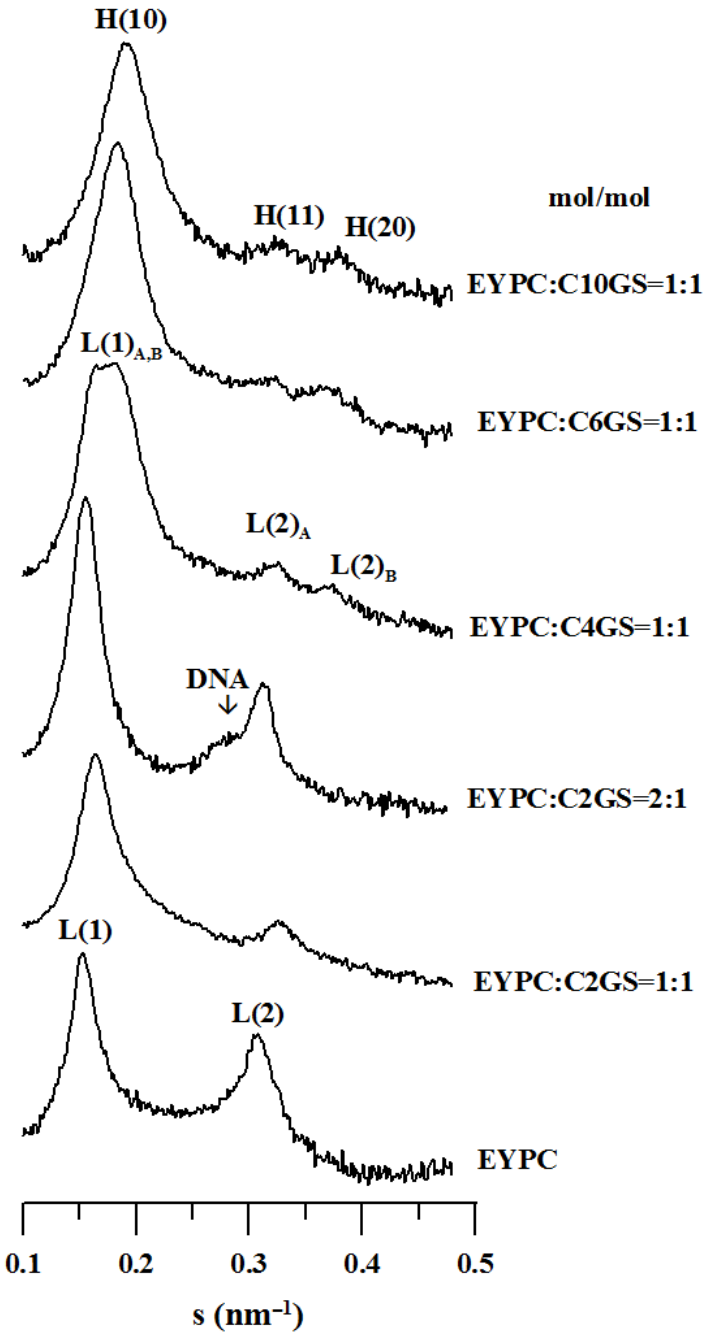

Fig. 2 SAXD patterns of DNA – EYPC - CnGS complexes at molar ratios EYPC:CnGS = 1 and EYPC: C2GS=2 at 20°C.

lamellar phase (d = 6.38 ± 0.01 nm), a small broad peak induced by regular packing of DNA strands between bilayers (38, 39, 25). DNA forms a smectic layer, and we determined the DNA-DNA periodicity d_{DNA} = 3.57± 0.02 nm, deconvoluting peaks in the range of s ~ 0.20 –

0.36 nm^{-1} by fitting the pattern as a superposition of two Lorentzians. The diffractogram is characteristic for a condensed lamellar phase L_α^C with DNA strands packed regularly between phospholipid bilayer, as originally introduced in (38,39). Keeping the molar ratio EYPC:CnGS = 1:1, we have observed further structural changes as a function of the spacer's length. The diffractogram of EYPC-C4GS complex was identified as a structure with the coexistence of two lamellar phases, where the deconvolution of $L(1)_{A,B}$ into two peaks gives periodicities $d_A = 6.25 \pm 0.02$ nm and $d_B = 5.25 \pm 0.02$ nm. Coexistence of two lamellar phases indicates some microscopic demixing in the mixture. Unilamellar EYPC-CnGS vesicles do not show long-range order, and thus do not contribute to the diffraction pattern. Macroscopically, the sample did not show any inhomogeneity or phase separation. We suppose the coexistence of both phases in one aggregate. Similar effect was reported in our previous study of DNA – C4GS and dilauroylphosphatidylcholine (DLPC) complexes (40). At molar ratio C4GS:DLPC≥0.35 diffractograms have shown in addition to L_α^C the presence of a second lamellar phase with the repeat distance $d \sim 5.31$ nm which slightly decreased with increasing concentration of C4GS. The phase was associated to a formation of microscopic domains enriched by surfactant molecules. In this study, we "dilute" cationic ammonium headgroups (R_4N^+) in the surface of membrane increasing the volume fraction of neutral (helper) lipid. Similarly to C2GS, also for EYPC:C4GS≥2, the system has shown the condensed lamellar phase. It should be noted that in all complexes above reported, the obtained periodicity d of L_α^C phase is smaller to the one observed for pure EYPC bilayer stacking. The positive surface charge of membrane induced by R_4N^+ results in the lateral bilayer expansion. This bilayer expansion and the mismatch between the lengths of hydrophobic parts of CnGS ($m = 12$ is the length of CnGS alkyl chains) and EYPC ($m = 17.8$ (32)) results in an increase in populations of gauche isomers in hydrocarbon chains and, consequently, in the bilayer thickness decrease (41). The DNA is considered to be packed tightly in the water gap of L_α^C phase, supposing the water gap thickness ~ 2.5 nm what corresponds to the diameter of hydrated DNA strands (39,42). We can attribute the differences in the repeat distances of DNA-EYPC-CnGS, $n = 2$–4, to the bilayer thickness decrease in complexes.

The next increase in n, has induced a massive structural changes. Diffractograms of complexes DNA-EYPC-CnGS, $n \geq 6$, at EYPC:CnGS = 1 mol/mol have shown reflections at reciprocal spacing ratios 1, √3, 2,… that are consistent with a two-dimensional hexagonal lattice. We have determined the lattice parameter $a = 2/(\sqrt{3}.s_{10}) = 6.31 \pm 0.01$ nm (s_{10} is the

position of the first order peak's maximum), characterizing the distance between the axes of two adjacent cylinders forming a columnar hexagonal phase. With increasing length of spacer n = 6–12, the lattice parameter a decreased nonlinearly, reaching the value a = 5.86± 0.01 nm in DNA-EYPC-C12GS complexes (not shown). Evidently, the length of CnGS spacer affects the curvature of the membrane surface. A defect created by an intercalation of C2GS into EYPC hydrophobic core is compensated by *trans-gauche* isomerizations of chains, and short spacer does not disturb the lamellar organization. Larger values of n correspond to a gradually more flexible spacer that is able to change its conformation in order to reduce the hydrocarbon–H_2O contact. Experiments described in (43,44) indicate a change of location of spacer from the interface, trying to push itself inside the hydrophobic core in order to minimize its contact with water. Small-angle neutron scattering study (45) has shown that CnGS (n = 8–12, m = 10) form a prolate ellipsoidal micelles in water. At molar ratio EYPC:CnGS=1:1, two cationic R_4N^+ groups are spanned with the spacer and separated by one headgroup of EYPC molecule. The flexibility of longer spacer (n = 6–12) and hydrophobic mismatch results in a formation of probably energetically more favourable, non-lamellar phase. Our experimental data do not allow to detect if complexes form condensed columnar inverted hexagonal phase (H_{II}^C) with linear DNA molecules surrounded by lipid monolayers (as observed in (46), and for DNA – gemini surfactants – dioleoylphosphatidylethanolamine (DOPE) in (29)), or an intercalated hexagonal structure (H_I), where each DNA strand is surrounded by three cylindrical micelles of EYPC-CnGS mixture (as it was found in (47,48)).

Our study was focussed to follow structural changes, particularly DNA-DNA packing in DNA-EYPC-CnGS complexes in a large range of molar ratios 1≤EYPC:CnGS≤10, n=2-12, prepared at DNA:CnGS=1 mol bp/mol. In the range of molar ratios 2≤EYPC:CnGS≤10, all studied complexes have shown the condensed lamellar phase L_α^C. Figure 3 shows an example of obtained diffractograms. We report structural changes in DNA-EYPC-C6GS as a function of surface charge density modulated through the volume fraction of neutral phospholipid. The increase of the EYPC volume fraction in the membrane, keeping the quantity of R_4N^+ groups constant, leads to the separation of positive charges and, to the decrease in surface charge density. It has been proven, that the effective surface charge density of membrane is responsible for d_{DNA} distance (24). Figure 3 shows the shift of the peak related to the DNA-DNA packing (marked by arrow) to the smaller s values with increasing molar ratio EYPC:C6GS, thus $d_{DNA}=1/s_{DNA}$ increased. At low molar ratio, EYPC:C6GS=2, a minute

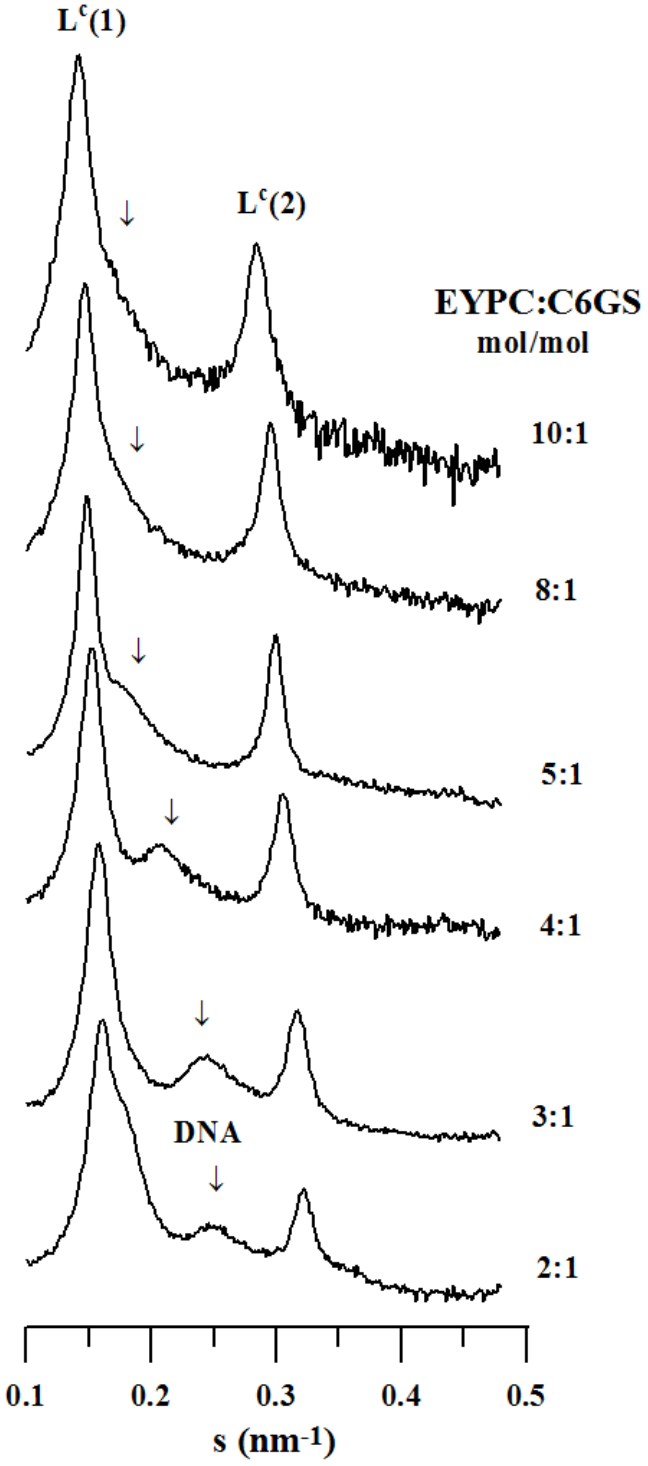

Fig. 3 SAXD patterns of DNA – EYPC – C6GS complexes as a function of EYPC:C6GS molar ratio (at 20°C). The peak related to DNA-DNA packing is marked by arrow.

asymmetry can be seen in the shape of the first peak at detailed inspection. We have identified this asymmetry in diffractograms at EYPC:CnGS = 2 mol/mol, n = 6–12. The deconvolution of the peak has revealed the presence of the next phase with periodicity d ~ 5.63 nm (in DNA-EYPC-C6GS complexes), close to that observed for the hexagonal phase (d = 5.45 nm) at EYPC:C6GS=1 mol/mol. Most probably a small volume of the mixture still adopts the organization of hexagonal symmetry. Structural parameters of L_α^C as a function of 2≤EYPC:CnGS≤10 molar ratios, n = 2–12, were obtained by fitting of diffraction peaks, as described in Materials and Methods. In Figure 4 dependences of d and d_{DNA} *vs.* EYPC:CnGS molar ratio (for n = 4–12) extracted from diffractograms are shown. The repeat distance d *vs.* EYPC:CnGS molar ratio has shown qualitatively the same course: We observe a non-linear increase in d up to molar ratio EYPC:CnGS ~ 5, the next increase in the EYPC volume fraction does not effect the bilayer periodicity in a marked way. This course corresponds well with the concept of hydrophobic mismatch due to differences in the length of alkyl/acyl chains of the surfactant and lipid molecules. Above the molar ratio EYPC:CnGS ≅ 5, the defect in hydrophobic core induced by shorter CnGS (m=12) alkyl chain is smaller, and d slightly increases with increasing volume fraction of EYPC. The d_{DNA} *vs.* EYPC:CnGS have shown different regimes of DNA packing in dependence on the spacer's length. We have found the linear dependence in d_{DNA} *vs.* EYPC:CnGS when complexes were prepared with CnGS homologues of short spacer, n = 2, 4 and with the longest spacer with n = 12 carbons (Figure 4, A and D). The linear dependence of d_{DNA} *vs.* EYPC:C2GS was reported in our previous study (28), where we found the increase in the DNA-DNA spacing, d_{DNA}, 0.39 ± 0.04 nm *per* 1 mol of EYPC from its slope. Complexes prepared with CnGS, n=6 and 10 have shown two ways in DNA packing as a function of EYPC:CnGS as shown in Figure 4, B and C. Generally, in all DNA-EYPC-CnGS complexes DNA strands move apart as a function of decreasing surface charge density of membrane. The gradient in DNA-DNA distance increase is almost the same in all complexes in the range of molar ratios 2≤EYPC:CnGS≤5. We determined the increase in d_{DNA} 0.40 ± 0.03 nm *per* 1 mol of EYPC from the slope of d_{DNA} = *f*(molEYPC/molCnGS). Thus the sufficiently high surface charge density "overlaps" the effect of the spacer's length in DNA-DNA packing. However, when the fraction of EYPC exceeds the molar ratio EYPC:CnGS ≅ 5, the CnGS spacers of intermediate length (n = 6–10) modulate the DNA-DNA distance, and allow closer approach of DNA strands in comparison to homologues with n = 2, 4 and 12. In complexes prepared with C8GS our experiment indicates a different way of DNA packing at EYPC:C8GS > 5 (Figure 4C, triangles) not

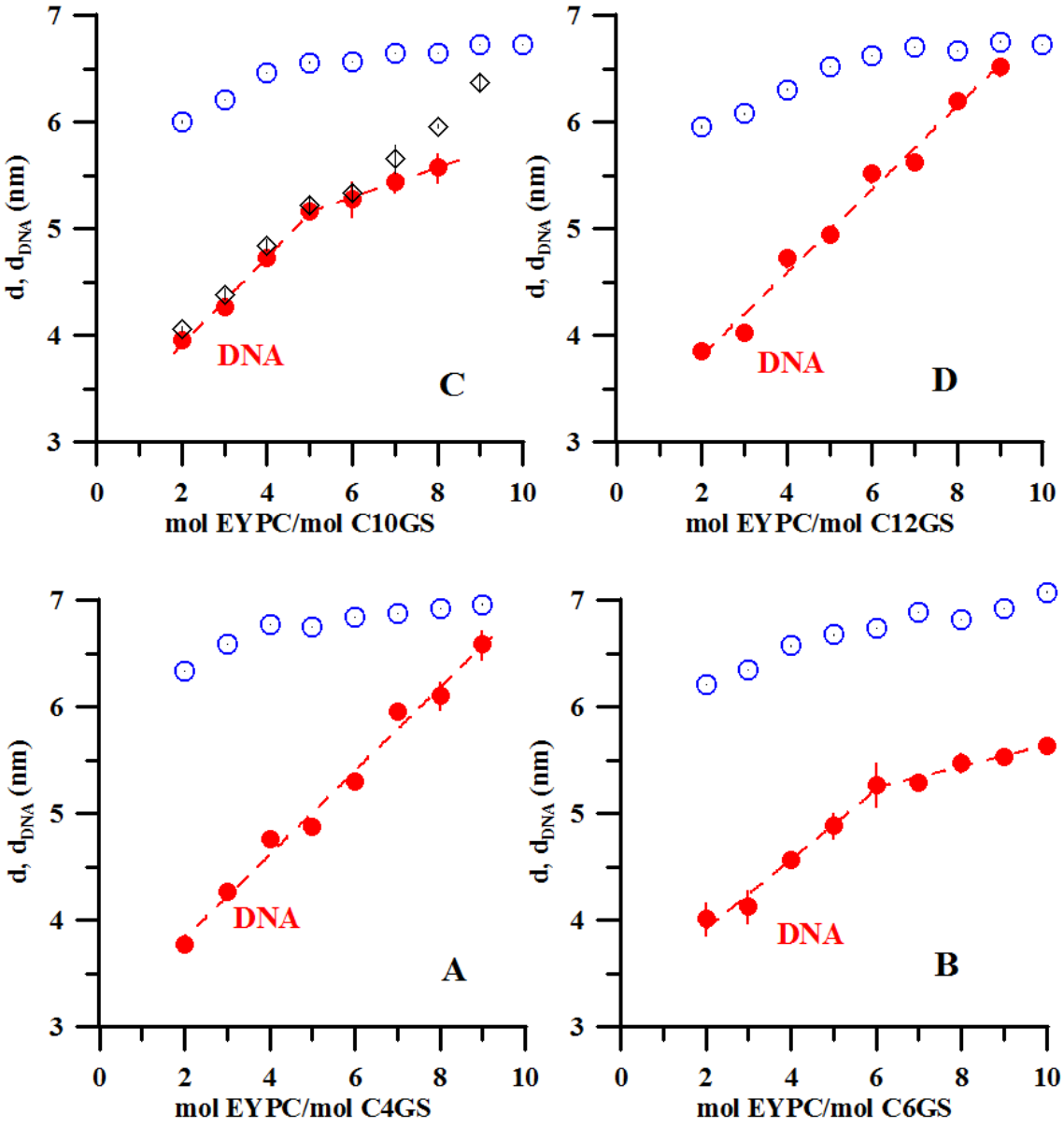

Fig. 4 The repeat distance *d* (○) and DNA interhelical distance d_{DNA} (●) *vs.* EYPC:CnGS molar ratio in DNA – EYPC – CnGS complexes at 20°C. (◊) d_{DNA} *vs.* EYPC:C8GS molar ratio in DNA – EYPC – C8GS complexes

consistent with any of the previous two. Although the relative surface charge density of R_4N^+ groups decreases due to GnGS dilution, the length and flexibility of the long spacer together with the lateral diffusion of CnGS in fluid membrane facilitate effective screening of DNA negative charges. At low surface charge density, EYPC:CnGS≥5, the arrangement of CnGS molecules with the spacer $n = 6 – 10$ in the plane of membrane allows closer approach of DNA strands, i.e. the length of CnGS spacer modulates the DNA - DNA distance. Complexes

prepared using CnGS with the longest spacer, n = 12, have shown the same slope in the *d vs.* EYPC:C12GS dependence as homologues with the short spacer, n = 2 and 4 (Figure 4, D and A). Thus the spacer with 12 carbons allows almost the same freedom in R_4N^+ groups arrangement in proximity of DNA as CnGS molecules with the short spacer (n = 2) that are assumed to act like a divalent cationic surfactants (49). We have shown the ability of CnGS to modulate the DNA-DNA distance in the range $3.57 \leq d_{DNA} \leq 6.59$ nm as a function of surface charge density and the length of the spacer. The linear dependence of d_{DNA} in L_α^C phase at isoelectric composition of the cationic liposomes – DNA mixture was predicted by (42). Koltover et al. (24) have observed a quasi-linear dependence of d_{DNA} with increasing the volume fraction of dioleoylphosphatidylcholine (DOPC) in a mixture of cationic lipid dioleoyl trimethylammonium propane (DOTAP) and DOPC, modulating the DNA-DNA distance in the range $2.46 \leq d_{DNA} \leq 5.71$ nm at the isoelectric composition. The lower limit, d_{DNA} = 2.46 nm was determined for complexes prepared with cationic lipid DOTAP itself. We got $d_{DNA} = 2.83 \pm 0.23$ nm by extrapolation of $d_{DNA} = f$(molEYPC/molC2GS) to zero volume fraction of EYPC. This value is close to diameter of hydrated DNA strand, ~ 2.5 nm (39). The authors (24) have reported coexistence of two phases at DOPC:DOTAP ~ 5 mol/mol relating this "demixing" to high volume fraction of DOPC ($\Phi_{PC} > 0.75$). Our diffractograms show no demixing in the range of EYPC volume fractions 0.37 – 0.92. Generally, demixing is associated to a formation of domains rich of cationic amphiphiles in proximity of DNA, and domains depleted of both, DNA and cationic amphiphiles (50,51), frequently observed at low surface charge density in systems cationic liposomes – DNA. Our recent experiments (52) showed that in addition to low surface charge density also the method of complex preparation and ionic strength of aqueous media are conditioning factors.

The effect of spacer in DNA-EYPC-CnGS complexes is illustrated in Figure 5, where we plot the structural parameters d and d_{DNA} as a function of the CnGS spacer's length at two selected molar ratios EYPC:CnGS=2 and 6, respectively. The dependence *d vs. n,* the CnGS spacer length, (Figure 5A) demonstrates the progressive decrease in the repeat distance with elongating spacer at constant molar ratio EYPC:CnGS. The polymethylene spacer contributes to the lateral expansion of the membrane, creating the defect in hydrophobic membrane's core effectively compensated by *trans-gauche* isomerisation of fluid chains, as discussed above. We have found the linear dependence in $d = f(n)$ showing the decrease in d, $\Delta d = d_{C2GS} - d_{C12GS}$ = 0.49 and 0.25 nm (±0.01 nm) at molar ratios EYPC:CnGS=2 and 6, respectively. Increasing volume fraction of EYPC reduces the defect in the hydrophobic core. At molar ratios

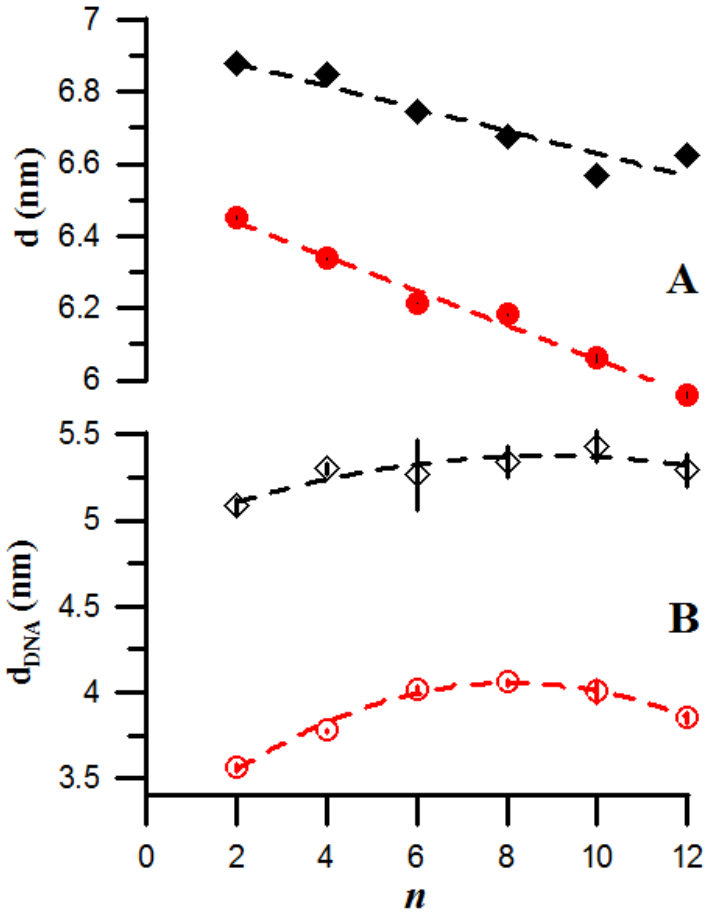

Fig. 5A,B The repeat distance *d* and DNA interhelical distance d_{DNA} as a function of the CnGS spacer length (*n*) at molar ratios EYPC:CnGS = 2 (●,○) and 6 (♦, ◊), at 20°C.

EYPC:CnGS≥7 we have observed a decrease in *d*, however the linear dependence was broken. Figure 5B shows the dependence of d_{DNA} as a function of the CnGS spacer's length at molar ratios EYPC:CnGS=2 and 6, respectively. The high surface charge density (EYPC:CnGS=2 mol/mol) allows for effective packing of DNA strands, and the plot shows non-linear increase in d_{DNA} with *n*. We found its variation in the range 3.57 – 4.06 nm (±0.02 nm), progressively increasing up to *n* = 6–8. Further elongating of the spacer does not lead to the increase in d_{DNA}. The high surface charge density allows effective arrangement of R_4N^+ groups in proximity of DNA. Our experiments do not allow to identify if the arrangement results from folding the long spacer into hydrophobic part of the membrane, or energetically favourable redistribution of R_4N^+ groups with the spacer protracted in the membrane's surface. Studies of polyamine – DNA complexes have shown that the spacing of 0.49 nm (equivalent to the trimethylene spacing in spermine) between amine groups is suitable to interact with adjacent phosphate groups of DNA (53). Wettig et al. (27) determined for CnGS

n = 3–16 the distance between N^+ - N^+ centres, l = 0.525 – 2.174 nm. A calculation of dimension of polar part of C12GS molecule with fully stretched spacer in vacuum (all-*trans* conformation) in (54) reports 2.11 nm and 0.42 nm for the longitudinal and the transversal distance supposing the shape of the area of the two polar ammonium heads linked by a spacer from the front view approximately rhomboidal. These intra-molecular dimensions are smaller in comparison to the DNA spacing determined in our experiment, however indicate sufficient freedom for R_4N^+ groups to adopt energetically and sterically favourable conformations. Also, one has to realise that R_4N^+ groups are not the only positively charged fragments in the membrane surface. The P^- - N^+ dipole of the phospholipid headgroup was referred to change its conformation for efficient screening of DNA phosphate groups in its condensation process (55,56). The DNA – DNA periodicity follows the surface charge density. We observe a marked increase in d_{DNA} at EYPC:CnGS=6 mol/mol and the dashed line indicates an intuitive course of the dependence (Figure 5B) that was broken at higher molar ratio (EYPC:CnGS≥7). It should be stressed that the obtained dependence $d_{DNA} = f(n)$ is conditioned by the high surface charge density, used phospholipid and DNA. For example we found recently the linear dependence of $d_{DNA} = 0.05n+3.50$ (nm) in DNA-DOPE-CnGS (n = 2–12) complexes at DOPE:CnGS=2.9 mol/mol that was broken at lower surface charge density (unpublished results).

Our experiments revealed no extremity in the DNA packing in DNA - EYPC – CnGS complexes with GS of short spacer in comparison to GS homologues of longer spacer related to the observed differences in their transfection effectivities. Lin et al. (14) found a high surface charge density of membrane (with optimum ~ e/100 Å^2) as a key parameter for transfection efficiency of L_α^C phase-forming complexes. The surface charge density of cationic liposomes depends on both, area per molecule of lipid and area per cationic additive. The area per CnGS molecule increases progressively with the length of spacer up to n ~ 12 (see e.g. 18, 54), i.e. molecules with two positive charges separated by the short spacer (n = 2, 3) should provide the optimal surface charge density at lower CnGS:EYPC molar ratio in comparison to homologues with the long spacer. However, because of the spacer's length and flexibility, the surface charge distribution is less predictable than in complexes with simple cationic molecules. Karlsson et al. (49) reported that the spacing between the two positive charges on the C2GS is so small that the surfactant acts like a divalent cationic surfactant at DNA compaction. Our recent experiments (ITC and zeta potential measurements) have detected the actual isoelectric point for DNA-DOPC-C2GS complexes in 5 mM NaCl at approximately two times higher ratio C2GS/DNA than the calculated isoelectric point (52).

The overcharging of the complex away from its isoelectric point is caused by changes of the bulk structure with absorption of excess DNA or cationic lipid (24). Other factors, like the increase in ionic strength reduces the amount of DNA which the cationic liposomes are able to bind (24,52,57), shifting the electro-neutrality to the higher ratio of +/- charges. Generally, it is believed that positively charged complexes are attached to the anionic cell surface and transfer DNA into the cell cytoplasm, either the negatively charged complexes for successful DNA deliver *in vivo* were reported as well (58).

Conclusion

DNA due to interaction with EYPC-CnGS (n = 2–12) vesicles forms the condensed lamellar phase in the range of molar ratios 2≤EYPC:CnGS≤10. The distance between adjacent DNA strands increases with decreasing surface charge density of EYPC-CnGS vesicles. Experimental results indicate that sufficiently high surface charge density (2≤EYPC:CnGS≤5 mol/mol) „masks“ the role of spacer, DNA strands move apart with the gradient in d_{DNA} 0.40 ± 0.03 nm *per* 1 mol of EYPC. At low surface charge density, EYPC:CnGS > 5 mol/mol, spacers of intermediate lenght, n = 6–10, modulate the DNA-DNA distance. The spacer with 12 carbons allows more-less the same freedom in R_4N^+ groups arrangement in proximity of DNA as CnGS with short spacer (n = 2). The high surface charge density (EYPC:CnGS=2 mol/mol) allows effective packing of DNA, and a non-linear increase in d_{DNA} with n is observed, showing the maximum at n = 6–8. Both, the short spacer of CnGS and the low molar ratio EYPC:CnGS provide a high surface charge density of membrane that was found as a key parameter for transfection efficiency of L_α^C phase-forming complexes (14).

Acknowledgements

Authors thank Prof. P. Balgavý for the challenging discussion of the subject and Assoc. Prof. I. Lacko for kindly providing the CnGS chemicals. Financial support provided by the European Community's Seventh Framework Program (FP7/2007-2013) under grant agreement no 226716 (HASYLAB project II-20100372 EC), and by project CEBV 26240120034, supported by the Research and Development Operational Programme funded by the ERDF is gratefully acknowledged.

Reference List

1. Imam T, Devínsky F, Lacko I, Mlynarčík D, Krasnec L. Preparation and antimicrobial activity of some new bisquaternary ammonium salts. Pharmazie 1983;38:308-310.

2. Devínsky F, Masarová L, Lacko I, Mlynarčík D. Bis-quaternary ammonium-salts 5. Synthesis, IR-spectra, and antimicrobial activity of some bis-ammonium salts of N,N'-bis(2-dimethylaminoethyl)methylamine. Coll Czech Chem Commun 1984;49:2819-2827.

3. Devínsky F, Lacko I, Bittererová F, Tomečková L. Relationship between structure, surface-activity, and micelle formation of some new bisquaternary isosteres of 1,5-pentanediammonium dipromides. J Colloid Interface Sci 1986;114:314-322.

4. Devínsky F, Masárová L, Lacko I. Surface-activity and micelle formation of some new bisquaternary ammonium-salts. J Colloid Interface Sci 1985;105:235-239.

5. Pisárčik M, Dubničková M, Devínsky F, Lacko I, Škvarla J. Dynamic light scattering and electrokinetic potential of bis(quarternary ammonium bromide) surfactant micelles as the function of the alkyl chain length. Coll Surf. A 1998;143:69-75.

6. Belicová A, Ebringer L, Devínsky F. Plasmid curing capacity of bisquaternary ammonium-salts – comparison of 4 sets of N,N'-bis(alkyldimethyl)-3-X-1,5-pentanediammonium dibromides. Biologisches Zentralblatt 1995;114:294-298

7. Horniak L, Devínsky F, Balgavý P, Lacko I, Ebringer L. Quaternary ammonium halides for increased efficiency of bacterial transformation. [Patent 88/3,560 (CS 269,549)]. 1990. Czechoslovakia.

8. Camilleri P, Kremer A, Edwards AJ, Jennings KH, Jenkins O, Marshall I, et al. A novel class of cationic gemini surfactants showing efficient in vitro gene transfection properties. Chem Commun 2000;1253-1254.

9. Bell PC, Bergsma M, Dolbnya IP, Bras W, Stuart MCA, Rowan AE, et al. Transfection mediated by gemini surfactants: Engineered escape from the endosomal compartment. J Am Chem Soc 2003;125:1551-1558.

10. Bombelli C, Giansanti L, Luciani P, Mancini G. Gemini Surfactant Based Carriers in Gene and Drug Delivery. Curr Med Chem 2009;16:171-183.

11. Kirby AJ, Camilleri P, Engberts JBFN, Feiters MC, Nolte RJM, Soderman O, et al. Gemini surfactants: New synthetic vectors for gene transfection. Angew Chem Int Ed 2003;42:1448-1457.

12. Felgner PL, Ringold GM. Cationic liposome – mediated transfection. Nature 1989;337:387-388.

13. Farhood H, Serbina N, Huang L. The role of dioleoylphosphatidylethanolamine in cationic liposome – mediated gene-trnasfer. Biochim Biophys Acta-Biomembranes 1995;1235:289-295.

14. Lin AJ, Slack NL, Ahmad A, George CX, Samuel ChE, Safinya CR. Three-dimensional imaging of lipid gene-carriers: Membrane charge density controls universal transfection behavior in lamellar cationic liposome-DNA complexes. Biophys J 2003;84:3307-3316.

15. Hirsch-Lerner D, Zhang M, Eliyahu H, Ferrari ME, Wheeler CJ, Barenholz Y. Effect of "helper lipid" on lipoplex electrostatics. Biochim Biophys Acta 2005;1714:71-84.

16. Masotti A, Mossa G, Cametti C, Ortaggi G, Bianco A, Del Grosso N, et al. Comparison of different commercially available cationic liposome–DNA lipoplexes: Parameters influencing toxicity and transfection efficiency. Coll Surf B 2009;68:136-144

17. Foldvari M, Badea I, Wettig SD, Verrall R, Bagonluri M. Structural characterization of novel gemini non-viral DNA delivery systems for cutaneous gene therapy. J Exp Nanosci 2006;1:165-176.

18. Badea I, Verrall R, Baca-Estrada M, Tikoo S, Rosenberg A, Kumar P, et al. In vivo cutaneous interferon-gamma gene delivery using novel dicationic (gemini) surfactant - plasmid complexes. J Gene Med 2005;7:1200-1204.

19. Jennings KH, Marshall ICB, Wilkinson MJ, Kremer A, Kirby AJ, Camilleri P. Aggregation properties of a novel class of cationic gemini surfactants correlate with their efficiency as gene transfection agents. Langmuir 2002;18:2426-2429.

20. Dass CR. Lipoplex-mediated delivery of nucleic acids: factors affecting in vivo transfection. J Mol Med 2004;82:579-591.

21. Cardoso AMS, Faneca H, Almeida JAS, Pais AACC, Marques EF, Pedroso de Lima MC, et al. Gemini surfactant dimethylene-1,2-bis(tetradecyldimethylammonium bromide)-based gene vectors: A biophysical approach to transfection efficiency. Biochim Biophys Acta 2011;1808:341-351.

22. Fisicaro E, Compari C, Duce E, Donofrio G, Rozycka-Roszak B, Woznyak E. Biologically active bisquaternary ammonium chlorides: Physico-chemical properties of long chain amphiphiles and their evaluation as non-viral vectors for gene delivery. Biochim Biophys Acta 2005;1722:224-233.

23. Gershon H, Ghirlando R, Guttman SB, Minsky A. Mode of formation and structural features of DNA cationic liposome complexes used for transfection. Biochemistry-USA 1993;32:7143-7151.

24. Koltover I, Salditt T, Safinya CR. Phase diagram, stability, and overcharging of lamellar cationic lipid-DNA self-assembled complexes. Biophys J 1999;77:915-924.

25. Uhríková D, Rapp G, Balgavý P. Condensed lamellar phase in ternary DNA – DLPC – cationic gemini surfactant system: A small-angle synchrotron X-ray diffraction study. Bioelectrochemistry 2002;58:87-95.

26. Caracciolo G, Caminiti R. Do DC-Chol/DOPE-DNA complexes really form an inverted hexagonal phase? Chem Phys Lett 2005;411:327-332.

27. Wettig SD, Verrall RE, Foldvari M. Gemini surfactants: A new family of building blocks for non-viral gene delivery systems. Current Gene Therapy 2008;8:9-23.

28. Uhríková D, Šabíková A, Hanulová M, Funari SS, Lacko I, Devínsky F, et al. The microstructure of DNA - EYPC - gemini surfactants aggregates: a small-angle X-ray diffraction study. Acta Fac Pharm Univ Comenianae 2007;54:198-208.

29. Pullmannová P, Uhríková D, Funari SS, Lacko I, Devínsky F, Balgavý P. Polymorphic phase behaviour of DNA - DOPE - gemini surfactant aggregates: a small angle X -ray diffraction. Acta Fac Pharm Univ Comenianae 2008;55:170-182.

30. Caracciolo G, Piotto S, Bombelli C, Caminiti R, Mancini G. Segregation and phase transition in mixed lipid films. Langmuir 2005;21:9137-9142.

31. Singleton WS, Gray MS, Brown ML. Chromatographically homogenous lecithin from egg phospholipids. J Am Oil Chem Soc 1969; 42:53-56.

32. Filípek J, Gelienová K, Kovács P, Balgavý P. Effect of lipid autoperoxidation on the activity of the sarcoplasmic reticulum (Ca2+-Mg2+)ATPase reconstituted into egg yolk phosphatidylcholine bilayers. Gen Physiol Biophys 1993;12:55-68.

33. MacDonald RC, MacDonald RI, Menco BPhM, Takeshita K, Subbarao NK, Hu LR. Small-volume extrusion apparatus for preparation of large, unilamellar vesicles. Biochim Biophys Acta 2001; 1061:297-303.

34. Roveri N, Bigi A, Castellani PP, Foresti E, Marchini M, Strocchi R. Study of rat tail tendon by x-ray diffraction and freeze-etching technics. Boll Soc Ital Biol Sper 1980;56:953-959.

35. Chapman D. The polymorphism of glycerides. Chem Rev 1962;62:433-453.

36. Kellens M, Meeussen W, Reynaers H. Crystallization and phase – transition studies of tripalmitin. Chem Phys Lipids 1990;55:163-178.

37. Haydon DA, Myers VB. Surface charge, surface dipoles and membrane conductance. Biochim Biophys Acta 1973;307:429-443.

38. Lasic DD, Strey H, Stuart MCA, Podgornik R, Frederik PM. The structure of DNA-Liposome Complexes. J Am Chem Soc 1997;119:832-833.

39. Radler JO, Koltover I, Salditt T, Safinya CR. Structure of DNA-cationic liposome complexes: DNA intercalation in multilamellar membranes in distinct interhelical packing regimes. Science 1997;275:810-814.

40. Uhríková D, Hanulová M, Funari SS, Lacko I, Devínsky F, Balgavý P. The structure of DNA-DLPC-cationic gemini surfactant aggregates: a small angle synchrotron X-ray diffraction study. Biophys Chem 2004;111:197-204.

41. Balgavý P, Devínsky F. Cut-off effects in biological activities of surfactants. Adv Colloid Interface Sci 1996;66:23-63.

42. Harries D, May S, Gelbart WM, Ben Shaul A. Structure, stability, and thermodynamics of lamellar DNA-lipid complexes. Biophys J 1998;75:159-173.

43. Devínsky F, Lacko I, Mlynarčík D, Račanský V, Krasnec L. Relationship between critical micelle concentrations and minimum inhibitory concentrations for some non-aromatic quaternary ammonium salts and amine oxides. Tenside Deterg 1985;22:10-15.

44. Alami E, Beinert G, Marie P, Zana R. Alkanediyl-Alpha,Omega-Bis(Dimethylalkylammonium Bromide) Surfactants. 3. Behavior at the Air-Water-Interface, Langmuir 1993;9:1465-1467.

45. Hattori N, Hirata H, Okabayashi H, Furusaka M, O'Connor CJ, Zana R. Small-angle neutron scattering study of bis(quaternary ammonium bromide) surfactant micelles in water. Effect of the long spacer chain on micellar structure. Colloid Polym Sci 1999; 277:95-100.

46. Koltover I, Salditt T, Radler JO, Safinya CR. An inverted hexagonal phase of cationic liposome-DNA complexes related to DNA release and delivery. Science 1998;281:78-81.

47. Uhríková D, Zajac I, Dubničková M, Pisárčik M, Funari SS, Rapp G, et al. Interaction of gemini surfactants butane-1,4-diyl-bis (alkyldimethylammonium bromide) with DNA. Coll Surf B 2005;42:59-68.

48. Krishnaswamy R, Mitra P, Raghunathan VA, Sood AK. Tuning the structure of surfactant complexes with DNA and other polyelectrolytes. Europhys Lett 2003;62:357-362.

49. Karlsson L, van Eijk MCP, Soderman O. Compaction of DNA by gemini surfactants: Effects of surfactant architecture. J Colloid Interface Sci 2002;252:290-296.

50. Mitrakos P, Macdonald PM. Polyelectrolyte molecular weight and electrostatically-induced domains in lipid bilayer membranes. Biomacromolecules 2000;1:365-376.

51. Macdonald PM, Crowell KJ, Franzin CM, Mitrakos P, Semchyschyn DJ. Polyelectrolyte-induced domains in lipid bilayer membranes: the deuterium NMR perspective. Biochemistry & Cell Biology 1998;76:452-464.

52. Pullmannová P, Bastos M, Bai G, Funari SS, Lacko I, Devínsky F, et al. The ionic strength effect on the DNA complexation by DOPC - gemini surfactants liposomes. Biophys Chem 2012; 160:35-45.

53. Ruiz-Chica J, Medina MA, Sanchez-Jimenez F, Ramirez FJ. Fourier transform Raman study of the structural specificities on the interaction between DNA and biogenic polyamines. Biophys J 2001;80:443-454.

54. Pisárčik M, Rosen MJ, Polakovičová M, Devínsky F, Lacko I. Area per surfactant molecule values of gemini surfactants at the liquid-hydrophobic solid interface. J Coll Interface Sci 2005;289:560-565.

55. May S, Ben Shaul A. Modeling of cationic lipid-DNA complexes. Curr Med Chem 2004;11:151-167.

56. Mengistu DH, Bohinc K, May S. Binding of DNA to zwitterionic lipid layers mediated by divalent cations. J Phys Chem B 2009;113:12277-82.

57. Lobo BA, Davis A, Koe G, Smith JG, Middaugh CR. Isothermal titration calorimetric analysis of the interaction between cationic lipids and plasmid DNA. Arch Biochem Biophys 2001;286:95-105.

58. Son KK, Tkach D, Hall KJ. Efficient in vivo gene delivery by the negatively charged complexes of cationic liposomes and plasmid DNA. Biochim Biophys Acta 2000;1468:6-10.